论著·神经科学

头颈部高压脉冲电流暴露致小鼠急性神经行为异常且伴随海马可逆性损伤及转录组改变

张文娟,邓 平,王 徽,陶嘉雯,陈思羽,罗 燕,皮会丰,余争平,高 鹏 陆军军医大学(第三军医大学)军事预防医学系军队劳动卫生学教研室,教育部电磁辐射医学防护重点实验室,重庆

[摘要] **目的** 电击可引起神经系统功能异常,但不同暴露部位所致急性神经行为异常的差异尚不清楚。本研究旨在比较头颈部、胸腹部及背部短时高压脉冲电流暴露对小鼠神经行为的影响,并基于海马转录组学探讨头颈部暴露诱发异常反应的潜在机制,为电击致神经系统损伤的风险评估提供实验依据。**方法** 6~8周龄SPF级雄性C57BL/6J小鼠,体质量约20 g,采用随机数字表法分为(n=10):对照组、头颈部暴露组、胸腹部暴露组和背部暴露组。暴露组小鼠于麻醉状态下接受相应部位高压脉冲电流暴露5 s,对照组给予同等时长声光刺激(其余操作与暴露组相同)。暴露结束后立即行惊厥评分和强直时间评估,麻醉苏醒2 h后进行步态分析。基于上述结果,对头颈部暴露组和对照组行旷场实验、明暗箱实验及高架十字迷宫实验,以评估自主活动与焦虑样行为。取海马行HE及尼氏染色以观察神经组织病理改变,并行海马神经递质组学检测及RNA-seq分析,测定神经递质含量、筛选差异表达基因。**结果** 与对照组相比,头颈部暴露组、胸腹部暴露组和背部暴露组均出现不同程度惊厥反应及步态异常,其中头颈部暴露组10只小鼠中有4只达到3级,6只达到4级;胸腹部暴露组10只小鼠中,1只达到3级;背部暴露组10只小鼠中,1只达到3级,1只达到4级;且头颈部暴露组强直持续时间明显长于胸腹部暴露组和背部暴露组(P<0.000 1)。头颈部高压脉冲电流暴露后,小鼠表现出短暂的焦虑样行为,具体表现为暴露后2.5 h、26.0 h和50.0 h进入开臂次数减少、开臂停留时间缩短,暴露后2.5 h和26.0 h旷场中心区停留时间减少、总运动距离降低、明箱探索次数减少及明箱停留时间减少(P<0.05)。随着时间延长,上述行为学异常逐渐恢复,至74.0 h时与对照组小鼠相比差异无统计学意义。海马形态学观察结果显示,头颈部暴露组CA1区和DG区神经元间隙增宽、尼氏体凝集及核固缩细胞数量增多(P<0.05)。神经递质组学结果显示,头颈部暴露组海马5-羟色胺和甲状腺激素水平明显升高(P<0.05),其余与急性应激相关的神经递质,如肾上腺素、多巴胺、谷氨酸、乙酰胆碱及组胺等未见明显异常。RNA-seq分析共鉴定出差异表达基因186个,其中上调93个、下调93个,主要富集于黏着斑、细胞外基质-受体相互作用、cGMP-PKG和PI3K-Akt等信号通路。**结论** 相较于胸腹部和背部,头颈部短时高压脉冲电流暴露更易引发急性神经行为异常。头颈部短时高压脉冲电流暴露可造成小鼠海马可逆性损伤,伴随组织结构与基因转录水平的异常改变,可作为电击致神经系统损伤风险评估的重要实验参考。

[关键词] 电击伤;海马;神经行为;转录组

[中图法分类号] R363.25;R647;R741.02 [文献标志码] A

[基金项目] 重庆英才计划"包干制"项目(cstc2024ycjh-bgzxm0102)

[通信作者] 高 鹏,E-mail:gaopeng999666@126.com

2097-0927/Copyright © 2026, 陆军军医大学(第三军医大学)。这篇开放获取文章遵循 CC BY 许可协议 (https://creativecommons.org/licenses/by/4.0/)

引用格式:张文娟,邓平,王徽,等. 头颈部高压脉冲电流暴露致小鼠急性神经行为异常且伴随海马可逆性损伤及转录组改变[J]. 陆军军医大学学报,2026,48(20):2849-2861. DOI:10.16016/j.2097-0927.202606007.

Citation:Zhang W J, Deng P, Wang H, *et al*. Acute neurobehavioral abnormalities induced by high-voltage pulsed current exposure to the head and neck in mice accompanied by reversible hippocampal injury and transcriptomic alterations[J]. J Army Med Univ, 2026, 48(20):2849-2861. DOI:10.16016/j.2097-0927.202606007.

Acute neurobehavioral abnormalities induced by high-voltage pulsed current exposure to the head and neck in mice accompanied by reversible hippocampal injury and transcriptomic alterations

Zhang Wenjuan, Deng Ping, Wang Hui, Tao Jiawen, Chen Siyu, Luo Yan, Pi Huifeng, Yu Zhengping, Gao Peng
Department of Occupational Health, Faculty of Military Preventive Medicine, Key Laboratory of Ministry of Education for Electromagnetic Radiation Protection, Army Medical University (Third Military Medical University), Chongqing, China

[**Abstract**] Objective Electric shock may cause neurological dysfunction, but the differences in acute neurobehavioral abnormalities induced by exposure to different body regions remain unclear. This study aimed to compare the effects of brief high-voltage pulsed current (HVPC) exposure to the head and neck, chest and abdomen, and back on neurobehavior in mice, and to explore the potential mechanism underlying the abnormal responses induced by head/neck exposure based on hippocampal transcriptomics, so as to provide an experimental basis for risk assessment of electrical shock-induced neurological damage. Methods Male SPF C57BL/6J mice (6 to 8 week old, weighing approximately 20 g) were randomly divided into 4 groups (n=10): control group, head/neck exposure group, chest/belly exposure group and back exposure group. Mice in the exposure groups were subjected to HVPC exposure at corresponding body regions for 5 s under anesthesia, while those in the control group received acoustic and light stimulation for same duration (with all other procedures identical to those of exposure groups). Seizure scores and tonic duration were assessed immediately after exposure, and gait analysis was performed at 2 h after anesthesia recovery. Based on the above results, open-field test, light-dark box test and elevated plus maze test were conducted in the head/neck exposure group and the control group to evaluate spontaneous locomotor activity and anxiety-like behaviors. Hippocampal tissues were harvested for HE and Nissl staining to examine neuropathological changes. Hippocampal neurotransmitter profiling and RNA-seq analysis were performed to detect neurotransmitter concentrations and screen differentially expressed genes (DEGs). Results Compared with the control group, the 3 exposure groups exhibited varying degrees of seizure responses and gait abnormalities. In the head/neck exposure group, 4 of 10 mice had seizure reaching grade 3 and 6 reaching grade 4; in the chest/belly exposure group, 1 mouse reached seizure grade 3; in the back exposure group, 1 mouse reached grade 3 and 1 reached grade 4. The tonic duration was significantly longer in the head/neck exposure group than the chest/belly and back exposure groups (P<0.000 1). After head/neck HVPC exposure, the mice demonstrated transient anxiety-like behaviors, manifested as decreased open-arm entry frequency and reduced open-arm residence time at 2.5, 26.0, and 50.0 h after exposure, decreased central zone residence time and total travel distance in the open-field test, as well as decreased entry frequency and residence time in the light compartment of light-dark box test at 2.5 and 26.0 h after exposure (P<0.05). These behavioral abnormalities gradually recovered over time, and no significant differences were observed relative to the control group at 74.0 h post-exposure. Morphological observation of the hippocampus found more widened neuronal gaps, condensed Nissl bodies and increased counts of karyopyknotic neurons in the CA1 and DG regions in the head/neck exposure group (P<0.05). Neurotransmitter profiling showed significantly elevated hippocampal 5-hydroxytryptamine and thyroid hormone levels (P<0.05), whereas no remarkable alterations in other acute stress-related neurotransmitters, such as epinephrine, dopamine, glutamate, acetylcholine and histamine in the head/neck exposure group. RNA-seq analysis identified a total of 186 DEGs, including 93 upregulated and 93 downregulated, which were mainly enriched in signaling pathways such as focal adhesion, extracellular matrix-receptor interaction, cGMP-PKG, and PI3K-Akt. Conclusion Compared with brief HVPC exposure to the chest and abdomen and the back, exposure to the head and neck is more likely to induce acute

neurobehavioral abnormalities. Such exposure can cause reversible hippocampal injury in mice, accompanied by abnormal changes in tissue structure and gene transcription levels, and may serve as an important experimental reference for the risk assessment of nervous system injury induced by electric shock.

[**Key words**] electric injuries; hippocampus; neurobehaviors; transcriptome

Supported by the "Lump Sum Contract" Project of Chongqing Talent Program (cstc2024ycjh-bgzxm0102). Corresponding author: Gao Peng, E-mail: gaopeng999666@126.com

电击可引起局部组织损害及心血管、呼吸、神经、肌肉等多个系统功能异常[1]。其生物学效应和影响因素,一直是法医学鉴定、损伤机制研究和安全防护评估关注的重点[2]。已有研究表明,电击损伤程度与电流参数、作用时间、接触方式及暴露部位等因素有关,但不同暴露部位所致神经系统效应的差异鲜有报道[3]。目前关于电击生物效应的研究多集中于其对皮肤、心血管系统、呼吸系统、骨骼肌及全身应激反应的影响[4-6],而电击后神经系统的损伤,特别是急性神经行为异常及其中枢机制尚缺乏系统研究。神经系统对电刺激敏感,急性电击暴露后机体易出现神经兴奋性紊乱、运动功能障碍、应激反应迟钝、惊厥发作及情绪行为异常等表现[7],因此阐明电击所致神经行为异常的特征及相关脑区的损伤机制,对完善电击损伤的致病理论具有重要价值。

海马参与学习记忆、空间定向、情绪调节与应激反应,对缺血缺氧、电生理紊乱和炎症等有害刺激高度敏感[8-9]。急性应激或有害刺激作用下,海马可发生神经元功能异常、突触可塑性改变及分子表达失衡,进而参与神经行为异常的发生[10]。因此,海马可能是电击后急性神经行为异常的中枢靶区,但其在电击损伤中的作用及分子基础尚不明确。

此外,暴露部位也是影响电击结局的重要因素。各部位解剖结构、神经分布、血管走行及毗邻关系不同,相同条件下产生的生物学效应也可能不同。靠近中枢或重要神经血管的区域,理论上更易诱发神经系统异常。然而,不同部位电击后急性神经行为异常是否存在差异,以及相关中枢机制,仍缺乏实验证据。

针对以上问题,本研究以C57BL/6J雄性小鼠为对象,建立不同部位短时高压脉冲电流暴露模型,比较不同暴露部位所致急性神经行为异常的差异,并结合惊厥评分、步态分析、海马组织形态学观察、神经递质检测及RNA-seq测序等方法,系统评估短时高压脉冲电流暴露后的神经行为学改变及海马转录组学特征,探讨其潜在分子机制。研究结果可为电击所致中枢神经系统损伤的机制阐释、临床风险评估及电气安全防护提供实验依据。

1 材料与方法

1.1 实验动物

6~8周龄SPF级C57BL/6J雄性小鼠,体质量约20 g,购自陆军军医大学实验动物中心,生产许可证号:SCXK(渝)2022-0011。所有实验动物饲养于独立通风笼盒内,适应性喂养1周。饲养环境温度控制在20~25 ℃,相对湿度50%~60%,光照周期采用12 h光照/12 h黑暗交替。饲养期间,小鼠自由摄食、饮水。为减轻实验动物的疼痛与不适,所有操作在充分麻醉或温和固定下实施。实验期间每日监测动物的精神状态、体质量及行为活动,详细记录不良事件。当动物体质量下降超过20%,出现严重精神萎靡或无法正常进食饮水时,及时实施安乐死以终止其痛苦。本研究实验设计、实验过程及动物处死方案均经陆军军医大学实验动物福利伦理审查委员会审核批准(AMUWEC20226182)。

1.2 主要仪器与试剂

主要仪器:高通量测序仪购自美国Illumina公司,荧光检测仪购自美国Thermo Fisher Scientific公司,CFX96荧光定量PCR仪购自美国Bio-Rad公司,光学显微镜购自德国Leica公司,低温高速离心机购自德国HERMLE公司。主要试剂:RNAiso Plus购自日本TaKaRa公司,Qubit RNA检测试剂盒购自美国Life Technologies公司,High Sensitivity DNA Kit购自美国Agilent Technologies公司,NEBNext Ultra™ RNA文库试剂盒购自美国NEB公司,氯仿、异丙醇、无水乙醇均购自中国川东化工公司。

1.3 方法

1.3.1 不同部位高压脉冲电流暴露模型建立与分组设计 采用随机数字表法将小鼠分为(n=10):对照组、头颈部暴露组、胸腹部暴露组和背部暴露组。所有小鼠按1.2 g/kg乌拉坦腹腔注射麻醉后固定,充分暴露相应部位并备皮。暴露组采用电警棍(K98型,江苏柯林,标称持续稳定输出电压20 kV)对相应部位持续电击5 s;对照组接受同等时长的声光刺激,其余操作(包括麻醉、固定、备皮及电极接触)与暴露组相同,以控制非暴露相关操作因素的潜在干扰[4]。暴露结束

后立即进行惊厥评分和强直时间评估,麻醉苏醒2 h后进行步态分析。基于以上筛查结果,选择头颈部暴露组与对照组,进一步进行行为学实验、海马组织形态学观察、神经递质组学和转录组学分析。

1.3.2 Racine标准评估惊厥反应和强直时间 高压脉冲电流暴露后由对分组不知情的观察者现场盲法观察小鼠惊厥发作情况,实时记录强直持续时间,并判断是否出现强直后肢伸展。惊厥发作严重程度依据Racine标准[11]分级,该标准按由轻至重的发作表现划分为0~5级:0级,无发作反应;1级,节律性口角、耳或面部肌肉抽动阵挛;2级,点头并伴随更严重的面部肌肉抽动阵挛;3级,前肢阵挛但不伴随直立;4级,前肢阵挛伴随直立;5级,全身强直阵挛发作而跌倒。

1.3.3 爪印实验观察不同部位高压脉冲电流暴露后小鼠的运动功能 该测试通过比较小鼠的步态模式来评估运动协调、平衡和共济失调。小鼠前后爪分别涂上无毒的红色和黑色油漆后,被放在1张白纸上,走过1条60 cm×10 cm×10 cm的通道。步态通过以下测量来评估:①连续后爪中心之间的步幅,即跨步长;②垂直于爪方向的后爪印之间的步幅,即步宽;③一侧成功前后爪印中心之间的足部重叠,即足迹重叠。每只小鼠每项参数共测量5次并进行分析[12]。

1.3.4 旷场实验(open-field test, OFT)、明暗箱(light-dark box, LDB)实验及高架十字迷宫(elevated plus maze, EPM)实验评估小鼠焦虑样行为 暴露组小鼠麻醉苏醒2 h后行OFT、LDB实验及EPM实验,并于暴露后2.5、26.0、50.0和74.0 h采用视频跟踪系统分别记录相应指标。OFT:将小鼠轻置于旷场中心,记录5 min自由活动,以旷场中心20 cm × 20 cm区域为中央区,统计中央区停留时间与总运动距离,中央区停留时间缩短提示小鼠出现焦虑样行为[13]。LDB实验:将小鼠置于明暗箱中央,允许其自由穿梭明、暗箱5 min,记录进入明箱次数及明箱停留时间,进入明箱次数减少、明箱停留时间缩短提示小鼠出现焦虑样行为[14]。EPM实验:迷宫由十字交叉的四臂组成,其中两臂为带30 cm高围墙的闭合臂(30 cm×10 cm),另两臂为开放臂(30 cm×10 cm),中央平台10 cm×10 cm,距地面40 cm,开放臂边缘设1.0 cm高唇缘以防跌落;实验在白色荧光灯照明房间内进行,将小鼠置于中央平台,视频跟踪记录5 min,记录开放臂停留时间及进入开放臂次数,开放臂停留时间越短、进入开放臂次数越少提示小鼠出现焦虑样行为[15]。

1.3.5 HE和尼氏染色观察头颈部高压脉冲电流暴露后小鼠海马形态学变化 上述实验结束后,将对照组和头颈部暴露组小鼠按1.2 g/kg乌拉坦腹腔注射麻醉后取海马,4%多聚甲醛固定24 h后,依次经70%、80%、90%、95%乙醇及无水乙醇(2次)梯度脱水(每级1~2 h),经二甲苯透明、石蜡浸渍后包埋,制备连续切片。切片依次经环保型脱蜡透明液Ⅰ、Ⅱ各15 min,无水乙醇Ⅰ、Ⅱ各5 min,75%酒精5 min脱蜡至水,自来水冲洗。经尼氏和苏木精-伊红染色后,使用标准光学显微镜观察其组织病理学及形态学变化。

1.3.6 转录组测序与神经递质组学检测海马转录组及神经递质水平改变 对头颈部暴露组与对照组小鼠海马组织进行神经递质组学和转录组学分析。由于海马组织体积有限,不同检测项目分配至不同批次的不同动物个体,各项目样本量差异为实际通过质控的有效样本数。转录组学由上海欧易生物医学科技有限公司完成,神经递质组学由武汉迈维代谢生物科技股份有限公司完成,检测平台、前处理流程、质控方法和定量标准参照已发表文献[4,16]。转录组测序包括RNA提取、文库构建、测序、原始数据质控、比对、差异表达分析以及GO和KEGG富集分析。差异表达基因筛选标准设定为$|\log_2FC|>1$,$P<0.05$。

1.4 统计学分析

采用SPSS 23.0软件进行统计学分析。计量资料用$\bar{x}\pm s$表示。多组间比较采用单因素方差分析(one-way ANOVA),方差齐时行LSD事后检验,方差不齐时采用Games-Howell检验;两组间比较采用独立样本t检验。$P<0.05$表示差异具有统计学意义。

2 结果

2.1 不同部位高压脉冲电流暴露均可诱发小鼠急性惊厥反应,其中头颈部暴露组最为明显

暴露前,小鼠均处于麻醉状态;暴露过程中,小鼠出现全身肌肉紧张、四肢强直甚至站立、眼球突出并伴充血,部分小鼠可见甩尾动作。暴露结束后,小鼠全身肌肉逐渐松弛,尾部变软,出现张口、深快喘气、非自主凝视、频繁点头、咀嚼及面部节律性抽动,部分小鼠头皮可见点状出血。Racine惊厥评分结果显示,与对照组相比,各暴露组均出现不同程度的惊厥反应,其中头颈部暴露组最为明显。头颈部暴露组10只小鼠中,4只达到3级,6只达到4级;胸腹部暴露组10只小鼠中,1只达到3级,0只达到4级;背部暴露组10只小鼠中,1只达到3级,1只达到4级;且头颈部暴露组强直持续时间明显长于胸腹部暴露组和背部暴露组($P<0.000\,1$,图1)。上述结果提示,不同部位高压脉冲电流暴露均可诱发小鼠急性惊厥反应,其中头颈部暴露反应最为显著。

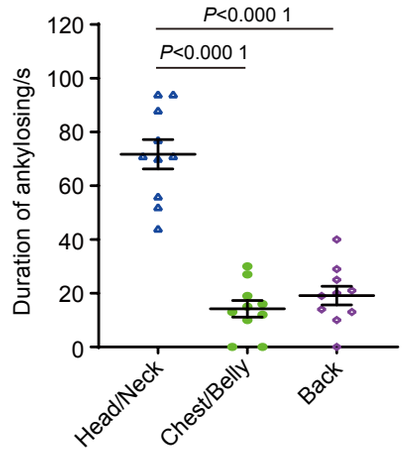
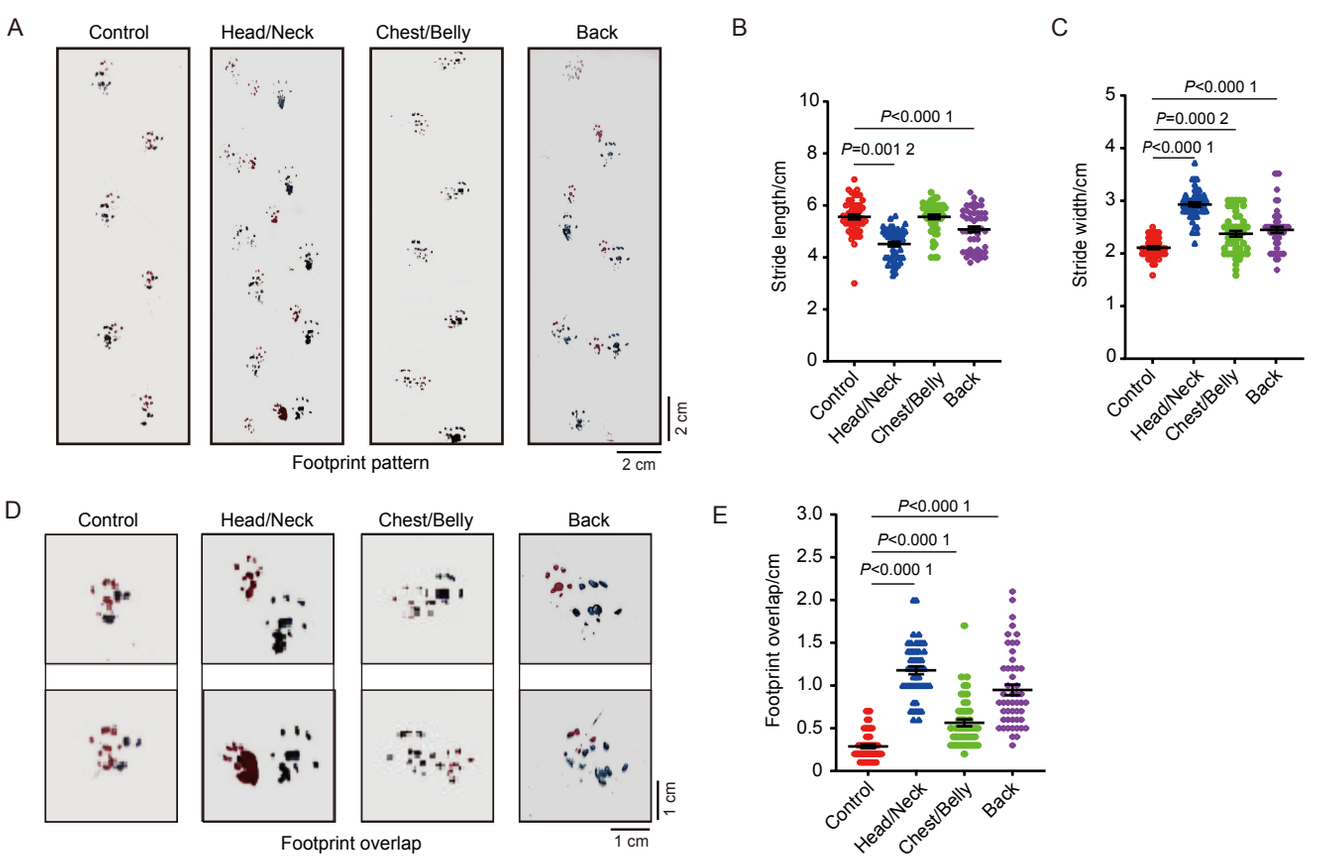


图1 不同部位高压脉冲电流暴露对小鼠强直时间的影响 (n=10, $\bar{x}\pm s$)

Figure 1 Effects of high-voltage pulse current (HVPC) exposure to different body regions on ankylosing duration in mice (n=10, $\bar{x}\pm s$)

2.2 不同部位高压脉冲电流暴露均可导致小鼠步态异常

步态分析结果显示,与对照组相比,头颈部暴露组、胸腹部暴露组和背部暴露组小鼠步态均发生明显改变。步长方面,头颈部暴露组(P=0.001 2)和背部暴露组(P<0.000 1)显著低于对照组(图2A、B);步宽方面,头颈部暴露组(P<0.000 1)、胸腹部暴露组(P=0.000 2)和背部暴露组(P<0.000 1)均显著高于对照组(图2C);足迹重叠方面,头颈部暴露组、胸腹部暴露组和背部暴露组均显著高于对照组(P<0.000 1,图2D、E)。该结果提示高压脉冲电流暴露可导致小鼠短时运动协调障碍。鉴于头颈部暴露组在惊厥评分实验中表现出最显著异常,后续行为学、海马组织病理学、神经递质组学及转录组学分析均选取头颈部暴露组与对照组进行比较。



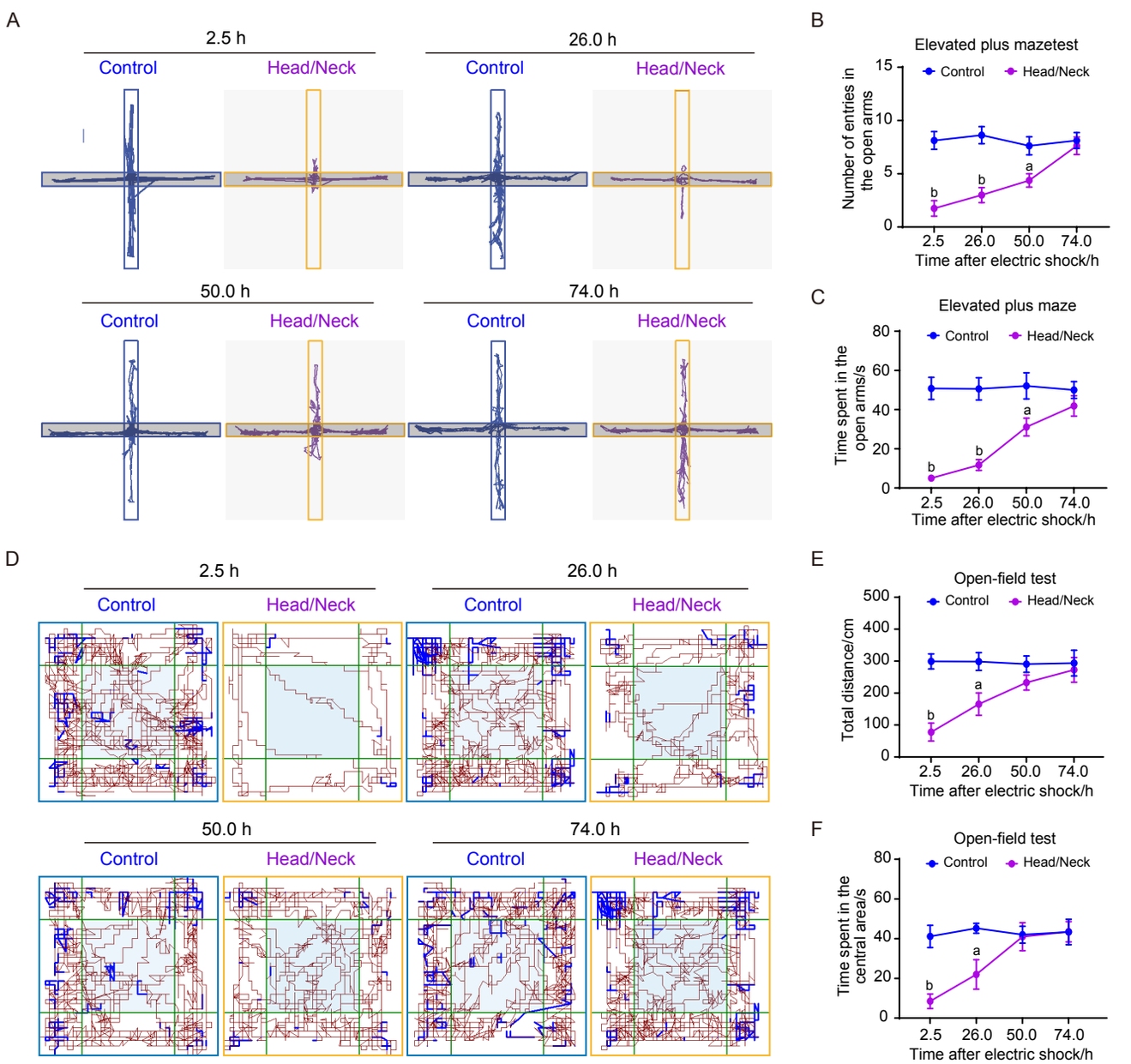
A: Representative footprint images of mice across groups; B: Quantitative scatter plot of stride length across groups; C: Quantitative scatter plot of stride width across groups; D: Schematic illustration for footprint overlap; E: Quantitative scatter plot of footprint overlap across groups. Forepaws are stained red and hindpaws are stained black

图2 不同部位高压脉冲电流暴露对小鼠步态的影响 (n=10, $\bar{x}\pm s$)

Figure 2 Effects of HVPC exposure to different body regions on gait parameters in mice (n=10, $\bar{x}\pm s$)

2.3　头颈部高压脉冲电流暴露可引起小鼠焦虑样行为并于74.0 h内逐渐恢复

行为学结果显示,头颈部高压脉冲电流暴露后,小鼠出现短暂焦虑样行为,具体表现为暴露后2.5 h、26.0 h和50.0 h进入开臂次数减少(P<0.05)、开臂停留时间缩短(P<0.05,图3A~C),暴露后2.5 h和26.0 h旷场中心区停留时间减少(P<0.05)、总运动距离降低(P<0.05)、明箱探索次数减少(P<0.01)及明箱停留时间减少(P<0.000 1,图3D~H)。随着时间延长,上述行为学异常逐渐恢复,至74.0 h时与对照组小鼠相比差异无统计学意义。该结果提示,高压脉冲电流暴露,尤其是头颈部暴露,可诱发短暂性焦虑样行为改变,且其影响在本研究观察时程内具有一定可逆性。

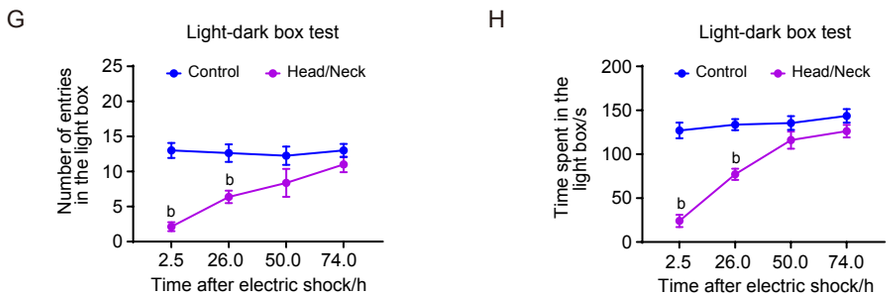


A: Representative track plot in the elevated plus maze test; B: Number of entries into the open arms; C: Time spent in the open arms; D: Representative track plot in the open field; E: Total distance moved; F: Time spent in the central zone. a: P<0.05, b: P<0.01, compared with the control group at the same time points

图3　头颈部高压脉冲电流暴露对小鼠焦虑样行为的影响 (n=10, $\bar{x}\pm s$)

Figure 3　Effects of HVPC exposure to the head and neck on anxiety-like behaviors in mice (n=10, $\bar{x}\pm s$)

(图3G、H续下页)



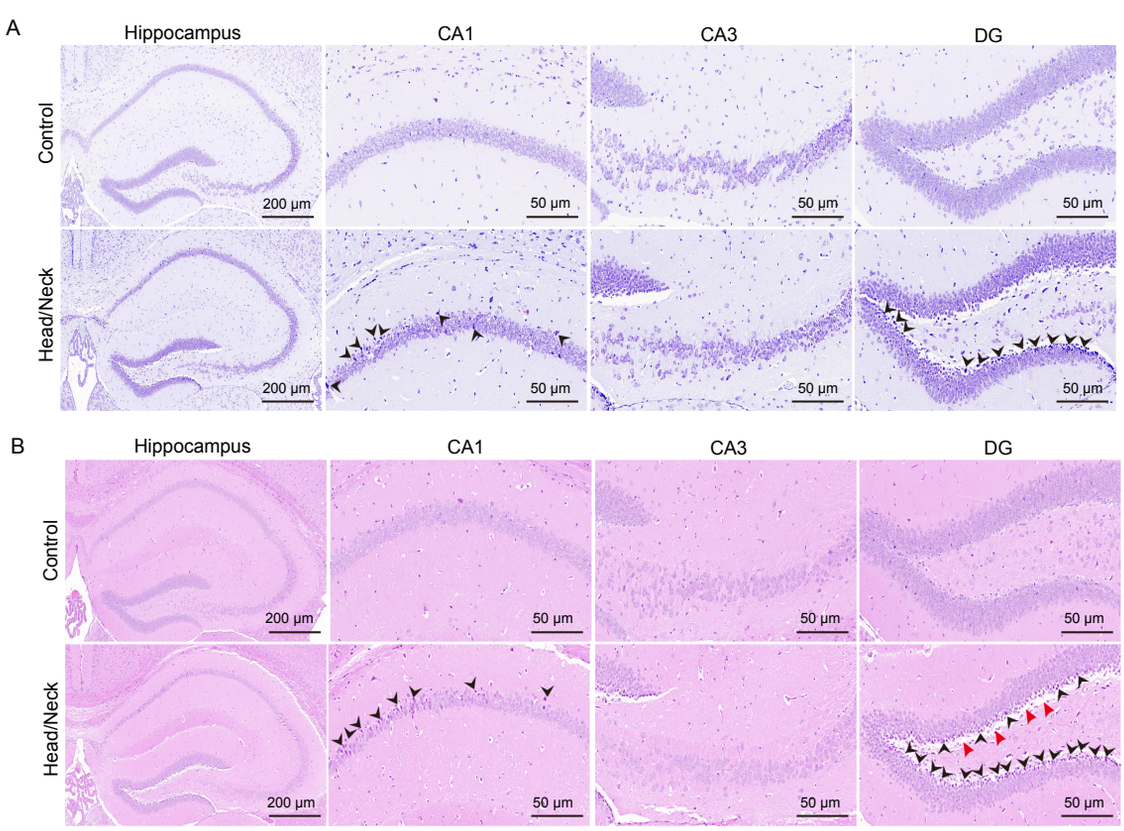
G: Number of entries into the light box; H: Time spent in the light box. a: $P<0.05$, b: $P<0.01$, compared with the control group at the same time points

续图3 头颈部高压脉冲电流暴露对小鼠焦虑样行为的影响(n=10, $\bar{x}\pm s$)

Figure 3(continued) Effects of HVPC exposure to the head and neck on anxiety-like behaviors in mice(n=10, $\bar{x}\pm s$)

2.4 头颈部高压脉冲电流暴露可导致海马CA1和DG区神经元形态改变

为进一步观察头颈部高压脉冲电流暴露后小鼠海马神经元形态学改变,本研究取对照组和头颈部暴露组小鼠海马组织进行尼氏染色和HE染色。结果显示,对照组小鼠海马CA1、CA3及DG区神经元排列相对整齐,细胞轮廓清晰,胞体形态较完整;而头颈部暴露组小鼠海马CA1和DG区可见神经元间隙增宽、细胞变形、尼氏体凝集,部分细胞出现核固缩(图4A、B)。定量分析结果显示,头颈部暴露组海马CA1区(P=0.009 9)及DG区(P<0.000 1)核固缩细胞数量较对照组均明显增加,CA3区核固缩细胞数量与对照组比较无明显差别(图4C~E)。上述结果表明,头颈部高压脉冲电流暴露可导致海马神经元急性形态学损伤。

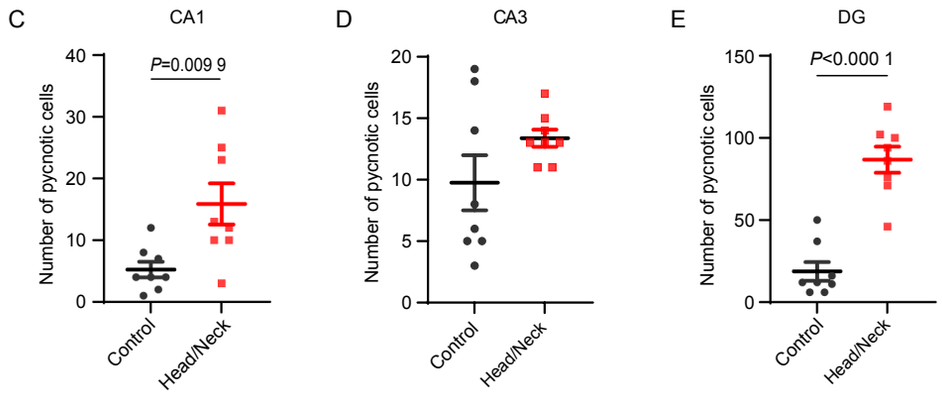


A: Representative images of Nissl staining. Black arrows indicate pyknotic cells; B: Representative images of HE staining. Red arrows indicate widened intercellular space, and black arrows indicate pyknotic cells

图4 头颈部高压脉冲电流对小鼠海马神经元形态学的影响(n=8, $\bar{x}\pm s$)

Figure 4 Effects of HVPC exposure to the head and neck on hippocampal neuronal morphology in mice(n=8, $\bar{x}\pm s$)

(图4C~E续下页)



C to E: Quantification of pyknotic cells in the CA1 (C), CA3 (D), and DG (E) subregions of the hippocampus in the head/neck exposure group and the control group

续图4　头颈部高压脉冲电流对小鼠海马神经元形态学的影响（n=8, $\bar{x}\pm s$）

Figure 4(continue)　Effects of HVPC exposure to the head and neck on hippocampal neuronal morphology in mice（n=8, $\bar{x}\pm s$）

2.5　头颈部高压脉冲电流暴露可明显增加海马5-羟色胺及甲状腺激素水平

利用神经递质组学对小鼠海马中55种神经递质进行分析,结果发现,与对照组相比,头颈部暴露组小鼠海马组织中5-羟色胺(P=0.013 1,图5A)和甲状腺激素水平(P=0.004 2,图5B)明显升高,提示头颈部暴露可引起小鼠海马神经化学稳态改变。其余与急性应激相关的神经递质,如肾上腺素、多巴胺、谷氨酸、乙酰胆碱及组胺等,未见明显改变。上述结果表明,头颈部高压脉冲电流暴露后海马神经递质改变具有一定选择性,而非全面性紊乱。

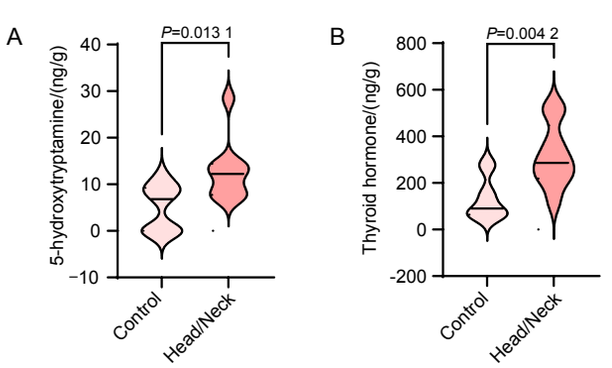


图5　头颈部高压脉冲电流暴露对小鼠海马5-羟色胺(A)及甲状腺激素(B)水平的影响（n=9, $\bar{x}\pm s$）

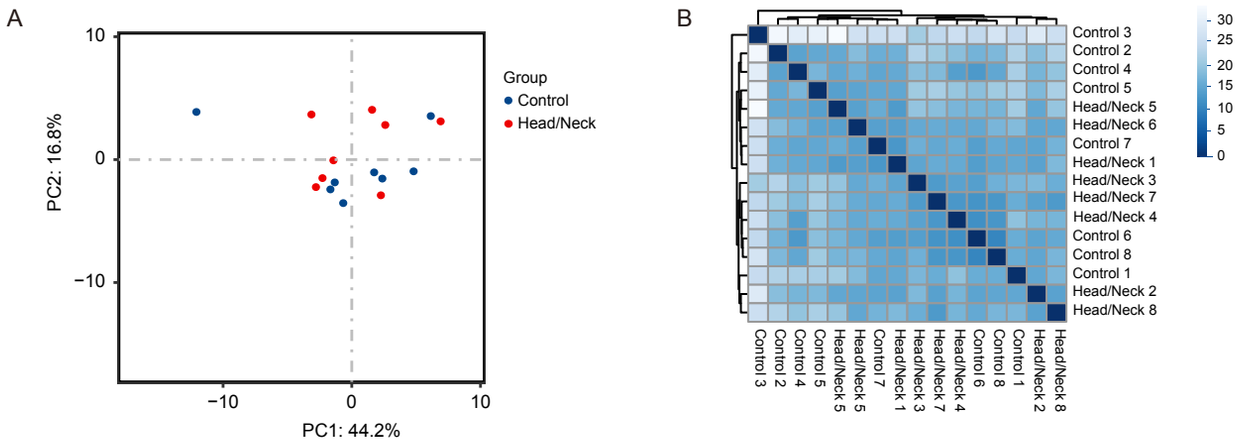
Figure 5　Effects of HVPC exposure to the head and neck on hippocampal 5-hydroxytryptamine (A) and thyroid hormone (B) levels in mice（n=9, $\bar{x}\pm s$）

2.6　头颈部高压脉冲电流暴露可改变海马转录组

2.6.1　样本质控分析　　为探讨头颈部高压脉冲电流暴露诱发小鼠急性神经行为异常的潜在分子机制,对对照组与头颈部暴露组小鼠海马组织进行RNA测序分析(n=8)。主成分分析(principal component analysis, PCA)结果显示,第一主成分和第二主成分的方差贡献率分别为44.2%和16.8%(图6A);2组样本在整体表达谱上表现出一定分离趋势,但仍存在部分样本交叉。相关性聚类分析显示组内样本相关性较好(图6B),表明测序数据整体质量可靠,可用于后续差异表达分析。

2.6.2　差异基因分析　　以$|\log_2 FC|>1$且$P<0.05$为筛选标准,共鉴定出186个差异表达基因(differentially expressed genes, DEGs),其中上调基因93个,下调基因93个。火山图显示了差异表达基因的整体分布特征(图7A),聚类热图显示对照组与头颈部暴露组在差异基因表达模式上的差异(图7B)。进一步按照$|\log_2 FC|$从大到小的顺序筛选表达变化前10的差异基因发现,上调基因包括Tmem252、Cd52、Timp1、Scgb3a1、Glycam1、Endou,下调基因包括Mybpc3、Fabp4、Tnnc1、Des(表1)。其中,Timp1、Glycam1等基因与细胞外基质(extracellular matrix, ECM)调节、细胞黏附相关,Cd52、Scgb3a1、Endou等基因可能参与免疫炎症及应激反应,提示头颈部高压脉冲电流暴露后小鼠海马组织可能存在细胞外基质调节、炎症/应激反应及细胞结构相关改变。

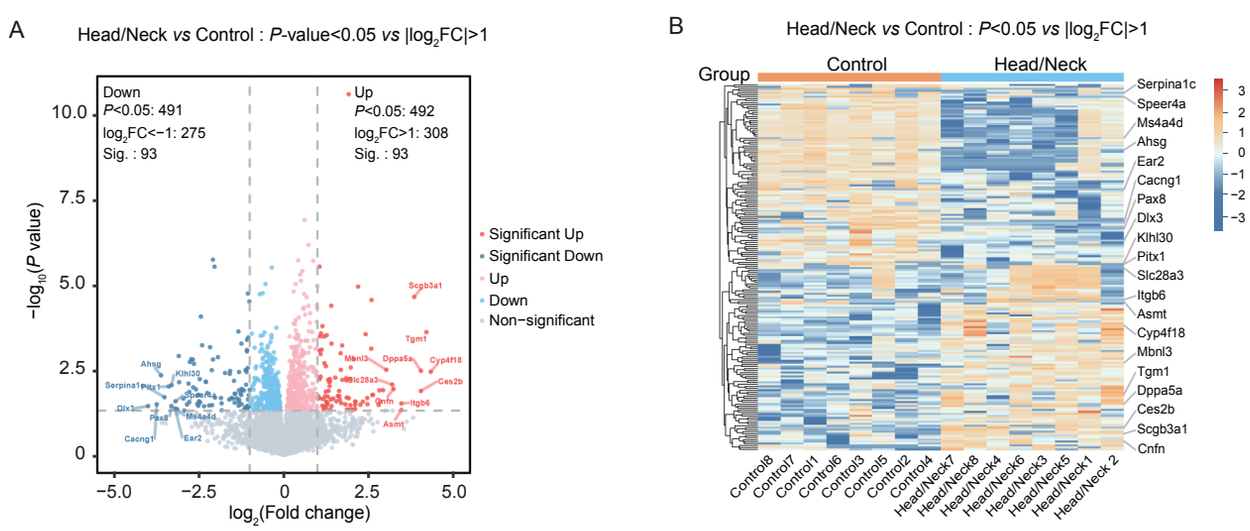
2.6.3　基因通路富集分析　　KEGG通路富集分析显示,差异表达基因主要富集于黏着斑、ECM-受体相互作用、cGMP-PKG信号通路、细胞黏附分子、PI3K-Akt信号通路及IL-17信号通路(图8)。其中,差异基因在黏着斑和ECM-受体相互作用等通路富集提示头颈部高压脉冲电流暴露可能影响海马细胞外微环境及细



A: Principal component analysis (PCA); B: Heatmap of correlation between samples

图6 头颈部高压脉冲电流暴露后小鼠海马转录组样本质控

Figure 6 Quality control of hippocampal transcriptome samples from mice after HVPC exposure to the head and neck



A: Volcano plot; B: Hierarchical clustering heatmap of differentially expressed genes

图7 头颈部高压脉冲电流暴露后小鼠海马差异表达基因分析

Figure 7 Differentially expressed gene analysis in the hippocampus of mice after HVPC exposure to the head and neck

表1 头颈部高压脉冲电流暴露后小鼠海马表达变化前10位的差异表达基因

Table 1 Top 10 differentially expressed genes (DEGs) in the hippocampus of mice after HVPC exposure to the head and neck

DEGs	Log_2FC	*P*	Regulation	Functional annotation
Tmem252	1.92	2.61×10^{-11}	Up	—
Mybpc3	−2.09	1.87×10^{-6}	Down	Cytoskeleton, muscle contraction or structural proteins
Fabp4	−2.04	3.00×10^{-6}	Down	Lipid metabolism and inflammatory regulation
Cd52	1.06	3.00×10^{-6}	Up	Immune regulation and inflammatory response
Timp1	2.20	1.15×10^{-5}	Up	Extracellular matrix degradation or alteration
Tnnc1	−1.05	1.84×10^{-5}	Down	Cytoskeleton, muscle contraction or structural proteins
Scgb3a1	3.85	2.31×10^{-5}	Up	Inflammatory regulation and tissue damage response
Glycam1	2.59	2.86×10^{-5}	Up	Cell adhesion and endothelial/immune cell migration
Des	−1.01	3.16×10^{-5}	Down	Cytoskeleton, muscle contraction or structural proteins
Endou	1.40	4.20×10^{-5}	Up	RNA metabolism and immune/inflammatory response

胞黏附状态;在cGMP-PKG和PI3K-Akt等信号通路的富集则提示神经元应激反应、细胞存活及功能调节相关分子事件可能参与其中。相关通路涉及的代表性差异基因见表2。

3 讨论

高压脉冲电流是电击伤的重要致伤因素,可造成心血管、神经、肌肉等多系统功能障碍。现有研究多聚焦于其对心、肝、皮肤等外周器官的损伤,而其对中枢神经系统的影响,尤其是不同暴露部位的神经效应差异及其分子机制尚不清楚。本研究通过比较不同部位高压脉冲电流暴露后小鼠神经行为差异和头颈部暴露后海马转录组改变,揭示了暴露部位在电击致神经系统损伤中的作用及潜在分子机制,为电击致神经系统损伤的风险评估与防控提供实验依据。

3.1 头颈部高压脉冲电流暴露更易诱发小鼠急性神经行为异常

本研究发现,不同部位(头颈部、胸腹部、背部)高压脉冲电流暴露均可诱发小鼠惊厥反应和步态异常,但以头颈部最为明显,提示暴露部位是电击致神经系统损伤的重要影响因素。头颈部邻近脑组织及重要感觉、运动传导通路,局部神经血管丰富,电流暴露更易累及中枢调控相关结构,从而更易引起神经功能异常[17]。临床亦有颈部电击致急性臂丛神经损伤、遗留

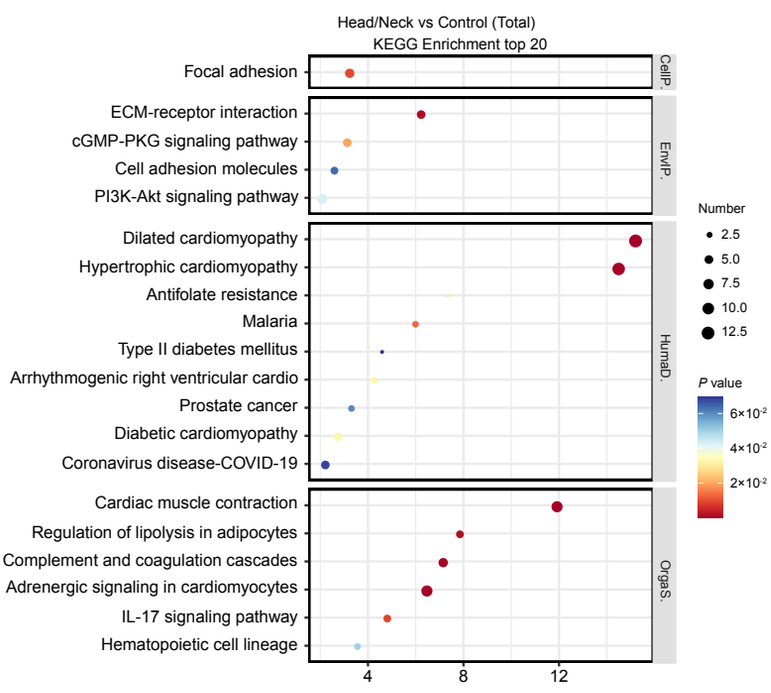


图8 头颈部高压脉冲电流暴露后小鼠海马差异表达基因的KEGG通路富集分析

Figure 8 KEGG pathway enrichment analysis of differentially expressed genes in the hippocampus of mice after HVPC exposure to the head and neck

表2 头颈部高压脉冲电流暴露后小鼠海马差异表达基因显著富集通路及对应基因

Table 2 Significantly enriched KEGG pathways and the corresponding genes among the differentially expressed genes in the hippocampus of mice after HVPC exposure to the head and neck

Pathway	Differentially expressed genes
Focal adhesion	Chad; Col2a1; Comp; Itgb6; Myl2; Myl7
ECM-receptor interaction	Cd36; Chad; Col2a1; Comp; Itgb6
cGMP-PKG signaling pathway	Ins2; Irs4; Myh6; Nppa; Pln
Cell adhesion molecules	Cd22; Cdh3; Cldn2; Glycam1
PI3K-Akt signaling pathway	Chad; Col2a1; Comp; Il7; Ins2; Itgb6; Prlr
IL-17 signaling pathway	Ccl12; Cxcl10; Mmp3; S100a9

长期肌无力的个案报道[18],进一步支持头颈部应作为电击伤风险防控的重点防护区域。

3.2 海马损伤及神经化学异常提示中枢神经系统参与头颈部高压脉冲电流暴露后的急性行为改变

组织形态学结果显示,头颈部高压脉冲电流暴露后,小鼠海马CA1、DG区出现神经元间隙增宽、细胞形态异常、尼氏体凝集和核固缩细胞增多,提示头颈部高压脉冲电流暴露可直接造成海马损伤。行为学检测发现,头颈部暴露可引起小鼠可逆性焦虑样行为改变,提示海马损伤与高压脉冲电流暴露后的急性神经行为紊乱有关。海马是参与情绪调节、应激反应及记忆加工的重要脑区,其结构损伤是焦虑及应激相关行为异常的重要病理基础[19]。已有研究显示,镉暴露、糖尿病等因素均可损伤海马神经元并导致认知功能障碍,与本研究海马损伤伴随行为异常的结果一致[20],支持海马结构损伤是中枢神经行为异常的重要诱因。

神经递质组学结果显示,头颈部高压脉冲电流暴露后,小鼠海马5-羟色胺和甲状腺激素水平显著升高,而多巴胺、谷氨酸、乙酰胆碱无明显变化。5-羟色胺参与情绪和应激反应调节,其升高多为急性应激状态下的代偿反应[21]。甲状腺激素对维持神经元兴奋性和神经系统稳态有重要作用[22]。本研究中神经化学指标的改变提示,头颈部高压脉冲电流暴露后的行为异常与海马中枢神经功能紊乱有关,而非单纯的外周电刺激所致。这也提示,临床电击伤的诊疗除评估外周肢体损伤外,还应关注患者情绪和认知功能的早期筛查与干预。

3.3 头颈部高压脉冲电流暴露后小鼠神经行为异常及海马损伤可能与细胞外基质改变及应激相关信号激活有关

头颈部高压脉冲电流暴露后小鼠海马共鉴定出186个差异表达基因,上调和下调各93个,提示头颈部高压脉冲电流暴露后小鼠海马转录组发生明显改变。富集分析显示,差异基因主要富集于黏着斑、ECM-受体相互作用、细胞黏附分子以及PI3K-Akt、cGMP-PKG、IL-17等应激和炎症相关通路。其中Timp1、Glycam1、Cd52、Scgb3a1等基因参与ECM重塑、细胞黏附调控和免疫应激反应,可能与高压脉冲电流暴露后的海马损伤有关。

已有研究显示,上述基因与通路在神经微环境稳态及损伤应答中发挥关键作用。Timp1编码的TIMP1蛋白是ECM稳态的核心调控因子,可通过抑制基质金属蛋白酶活性来平衡ECM降解与重塑,其异常表达可扰乱细胞黏附功能[23]。Glycam1作为ECM相关糖蛋白,可介导细胞黏附互作,参与组织微环境重塑过程[24]。Cd52与Scgb3a1为重要的免疫应激调控分子,可通过调控炎症反应、氧化应激及免疫细胞浸润参与神经损伤病理进程[25]。在通路方面,黏着斑和ECM-受体相互作用是细胞感知微环境、调控黏附与分化的主要途径,并能经PI3K-Akt通路影响细胞存活和损伤应答[26];cGMP-PKG通路参与ECM重塑,其活性异常与ECM病理性沉积有关[27];IL-17通路则通过放大炎症、诱导基质金属蛋白酶表达,同时影响神经炎症和ECM结构[28]。

本研究结果与上述文献证据一致,提示头颈部高压脉冲电流暴露所致的小鼠海马损伤和神经行为异常,并非单纯神经元损伤导致,还涉及ECM结构和细胞黏附功能紊乱、神经炎症和氧化应激通路的激活等多个环节。电击可能通过改变上述基因的表达,扰乱ECM和细胞黏附,激活炎症和应激信号,破坏海马微环境稳态,最终引起神经功能异常。

本研究存在一定局限性。首先,实验采用乌拉坦麻醉实施电击,虽可固定刺激部位、统一暴露条件、减少机械干扰,但乌拉坦会影响$GABA_a$、甘氨酸、NMDA及AMPA受体功能,改变神经元对电刺激的反应阈值,使神经激活模式与清醒状态存在差异,而低估高压脉冲电流的神经损伤效应[29]。其次,本研究仅采用单一电击参数和暴露时长,尚不能揭示不同刺激条件下的剂量-效应关系。再次,海马组学分析仅针对头颈部暴露组,难以充分解释不同部位暴露的差异机制。最后,本研究观察周期有限,无法评估远期神经行为学改变,关键差异基因及通路亦缺乏蛋白水平与功能学实验佐证。后续研究可利用清醒动物模型,探究不同部位高压脉冲电流暴露的神经行为学差异;设置多梯度刺激参数,明确剂量-效应关系与安全边界;延长观察周期评价远期效应。对候选差异基因开展蛋白表达检测,结合基因敲减、药理学干预等功能实验,构建转录改变与表型的因果关联,以进一步阐明海马在头颈部电击所致神经行为异常中的特异性作用。

综上,本研究表明,在相同实验条件下,不同部位高压脉冲电流暴露致急性神经行为异常的风险存在差异,其中头颈部风险更高,可诱发更明显的惊厥反应,同时伴随短暂性焦虑样行为、海马神经元形态学改变、5-羟色胺和甲状腺激素升高以及转录组改变。差异表达基因主要富集于细胞外基质-受体相互作用、黏着斑、PI3K-Akt和cGMP-PKG等通路,提示海马微环境改变及应激相关信号异常可能共同参与这一过程。

虽然本研究存在的诸多不足和局限性,使得研究结果外推受限,但是上述结果仍可为认识电击伤所致急性神经系统损伤提供实验依据,为相关损伤风险评估提供参考。

利益冲突 本文所有作者声明不存在利益冲突

参考文献:

[1] Smith I, Kidd S, Kim S, *et al*. Assessment and management of electrical injuries in adults in the emergency department [J]. Cureus, 2026, 18(4): e107162. DOI: 10.7759/cureus.107162.

[2] Jin X, Chen D Q, Li X B, *et al*. Advances in forensic diagnosis of electric shock death in the absence of typical electrical marks[J]. Int J Legal Med, 2021, 135(6): 2469-2478. DOI: 10.1007/s00414-021-02658-0.

[3] Schissler K, Pruden C. Pediatric electrical injuries in the emergency department: an evidence-based review[J]. Pediatr Emerg Med Pract, 2021, 18(12): 1-24.

[4] Zhang W J, Yin L C, Wang H, *et al*. Multiomics analysis elucidated the role of inflammatory response and bile acid metabolism disturbance in electric shock-induced liver injury in mice[J]. Chin J Traumatol, 2026, 29(1): 47-58. DOI: 10.1016/j.cjtee.2024.08.011.

[5] 罗燕, 王徽, 岳洋, 等. 基于代谢组学研究电击伤所致小鼠心肌损伤的效应研究[J]. 广西医科大学学报, 2024, 41(7): 952-958. DOI: 10.16190/j.cnki.45-1211/r.2024.07.002.
Luo Y, Wang H, Yue Y, *et al*. Study on the effect of myocardial injury induced by electrical injury in mice based on metabolomics[J]. J Guangxi Med Univ, 2024, 41(7): 952-958. DOI: 10.16190/j.cnki.45-1211/r.2024.07.002.

[6] 杨潇, 邓平, 陈思羽, 等. 基于代谢组学研究高压电击后小鼠皮肤损伤的特点和机制[J]. 局解手术学杂志, 2025, 34(5): 379-385. DOI: 10.11659/jjssx.04E024074.
Yang X, Deng P, Chen S Y, *et al*. Study on the characteristics and mechanisms of skin damage in mice after high-voltage electric shock based on metabolomics[J]. J Reg Anat Oper Surg, 2025, 34(5): 379-385. DOI: 10.11659/jjssx.04E024074.

[7] Yiannopoulou K G, Papagiannis G I, Triantafyllou A I, *et al*. Neurological and neurourological complications of electrical injuries[J]. Neurol Neurochir Pol, 2021, 55(1): 12-23. DOI: 10.5603/JNNS.a2020.0076.

[8] Nosratiyan N, Ghasemi-Kasman M, Pourghasem M, *et al*. Plumbagin improves cognitive function *via* attenuating hippocampal inflammation in valproic acid-induced autism model[J]. Brain Sci, 2025, 15(8): 798. DOI: 10.3390/brainsci15080798.

[9] Chen B, Liu Y J, Cai Y R, *et al*. Hippocampus is more vulnerable to neural damages induced by repeated sevoflurane exposure in the second trimester than other brain areas[J]. ABBS, 2020, 52(8): 864-874. DOI: 10.1093/abbs/gmaa060.

[10] Gao S F, Zhang L Y, Wang X, *et al*. A terrified-sound stress causes cognitive impairment in female mice by impairing neuronal plasticity[J]. Brain Res, 2023, 1812: 148419. DOI: 10.1016/j.brainres.2023.148419.

[11] 谢炜, 梁一超, 陈伟军, 等. 柴胡黄芩配伍应用对小鼠急性癫痫模型的影响[J]. 世界科学技术-中医药现代化, 2013, 15(2): 210-214. DOI: 10.11842/wst.2013.02.010.
Xie W, Liang Y C, Chen W J, *et al*. Effect of *Radix* bupleuri and *Radix* scutellariae in compatibility on acute epileptic mice model[J]. World Sci Technol Mod Tradit Chin Med, 2013, 15(2): 210-214. DOI: 10.11842/wst.2013.02.010.

[12] Ho R X, Amraei R, De La Cena K O C, *et al*. Loss of MINAR2 impairs motor function and causes Parkinson's disease-like symptoms in mice[J]. Brain Commun, 2020, 2(1): fcaa047. DOI: 10.1093/braincomms/fcaa047.

[13] Li Y D, Luo Y J, Xu W, *et al*. Ventral pallidal GABAergic neurons control wakefulness associated with motivation through the ventral tegmental pathway[J]. Mol Psychiatry, 2021, 26(7): 2912-2928. DOI: 10.1038/s41380-020-00906-0.

[14] Kuang X J, Zhang C Y, Yan B Y, *et al*. P2X2 receptors in pyramidal neurons are critical for regulating vulnerability to chronic stress[J]. Theranostics, 2022, 12(8): 3703-3718. DOI: 10.7150/thno.72144.

[15] Pi G L, Gao D, Wu D Q, *et al*. Posterior basolateral amygdala to ventral hippocampal CA1 drives approach behaviour to exert an anxiolytic effect[J]. Nat Commun, 2020, 11: 183. DOI: 10.1038/s41467-019-13919-3.

[16] Carreño F, Helfer V E, Staudt K J, *et al*. Quantification of neurotransmitters in microdialysate samples following quetiapine dosing to schizophrenia phenotyped rats using a validated LC-MS/MS method[J]. J Chromatogr B, 2020, 1155: 122282. DOI: 10.1016/j.jchromb.2020.122282.

[17] Cherington M. Central nervous system complications of lightning and electrical injuries[J]. Semin Neurol, 1995, 15(3): 233-240. DOI: 10.1055/s-2008-1041028.

[18] Brasholt M, Aon M, Michaelsen L, *et al*. Health impact of electric discharge weapons: a review of case studies[J]. Torture, 1970, 34(1): 48-61. DOI: 10.7146/torture.v34i1.144572.

[19] Illouz H, Menger Y, Schaack O, *et al*. Sex-specific spatial memory deficits associated with region-specific

neuroinflammatory changes in the dorsal hippocampus of rats exposed to neonatal repeated maternal separation[J]. Brain Behav Immun, 2025, 129: 388-398. DOI: 10.1016/j.bbi.2025.06.031.

[20] 史岩, 杨斯琪, 王友刚, 等. BDNF-TrkB信号通路在生命早期镉暴露致小鼠认知功能障碍中的作用[J]. 环境与职业医学, 2024, 41(11): 1283-1289. DOI: 10.11836/JEOM24045.
Shi Y, Yang S Q, Wang Y G, *et al*. Role of BDNF-TrkB signaling pathway in early-life cadmium exposure induced cognitive dys-function in mice[J]. J Environ Occup Med, 2024, 41(11): 1283-1289. DOI: 10.11836/JEOM24045.

[21] Bai S, Ying Z M, Ying J K, *et al*. Inhibition of 5-HT alleviates PTSD-like behaviors and promotes hippocampal neuroplasticity by modulating hippocampal autophagy in rats[J]. J Neurophysiol, 2024, 132(3): 979-990. DOI: 10.1152/jn.00291.2024.

[22] Samuels M H. Psychiatric and cognitive manifestations of hypothyroidism[J]. Curr Opin Endocrinol Diabetes Obes, 2014, 21(5): 377-383. DOI: 10.1097/MED.0000000000000089.

[23] Song G H, Xu S F, Zhang H, *et al*. TIMP1 is a prognostic marker for the progression and metastasis of colon cancer through FAK-PI3K/AKT and MAPK pathway[J]. J Exp Clin Cancer Res, 2016, 35(1): 148. DOI: 10.1186/s13046-016-0427-7.

[24] Klamer S, Voermans C. The role of novel and known extracellular matrix and adhesion molecules in the homeostatic and regenerative bone marrow microenvironment[J]. Cell Adh Migr, 2014, 8(6): 563-577. DOI: 10.4161/19336918.2014.968501.

[25] Rashidi M, Bandala-Sanchez E, Lawlor K E, *et al*. CD52 inhibits Toll-like receptor activation of NF-κB and triggers apoptosis to suppress inflammation[J]. Cell Death Differ, 2018, 25(2): 392-405. DOI: 10.1038/cdd.2017.173.

[26] Yang L, Wang M X, Hu X E, *et al*. EccDNA-oriented *ITGB7* expression in breast cancer[J]. Ann Transl Med, 2022, 10(24): 1344. DOI: 10.21037/atm-22-5716.

[27] Wang Y J, Zeng H, Li Z L, *et al*. Temporal transcriptomics leads from discovery to *in vivo* validation: COL4A3/COL4A6/COL4A5 and ITGA8 as novel arthrofibrosis biomarkers in post-traumatic joint contracture[J]. Dose Response, 2026, 24(1): 15593258261424570. DOI: 10.1177/15593258261424570.

[28] Chen M K, Zhu X F, Gao Q M, *et al*. Hemin activates interleukin-17 signaling and CCAAT/enhancer-binding protein beta to promote neuroinflammation and blood-brain barrier disruption[J]. Int J Biol Macromol, 2026, 366: 152476. DOI: 10.1016/j.ijbiomac.2026.152476.

[29] Hara K, Harris R A. The anesthetic mechanism of urethane: the effects on neurotransmitter-gated ion channels[J]. Anesth Analg, 2002, 94(2): 313-318, tableofcontents. DOI: 10.1097/00000539-200202000-00015.

(收稿:2026-06-02;修回:2026-09-03)

(编辑 刘秋池)